Current Continuity in Auroral System Science: Defining Electron Precipitation

J. van Irsel[1] (Jules.van.Irsel.gr@Dartmouth.edu), B. Francis Jr.[1], M. Conneely[1], A. Mule[1], S. R. Kaeppler[2], M. D. Zettergren[3], K. A. Lynch[1]; **MITC-14**

[1]Dept. of Physics and Astronomy, Dartmouth College; [2]Dept. of Physics and Astronomy, Clemson University; [3]Physical Sciences Dept., Embry-Riddle Aeronautical University

2023 CEDAR Workshop
San Diego, CA
25 - 30 June

Background

- Local auroral coupling of the ionosphere and magnetosphere (MI) is an open area of study (Wolf, 1975; Cowley, 2000; Lotko 2004; Amm et al. 2008).
- MI coupling demands self-consistent, topside maps of field-aligned current (FAC) and $\mathbf{E}\times\mathbf{B}$ plasma flow that agree with ionospheric conductivity patterns created by charged particle auroral precipitation.
- Discrete auroral precipitation provided by the auroral acceleration region creates arc-scale morphology in the ionospheric conductivity volume to which the MI coupling is highly sensitive.
- Quasi-static ionospheric plasma flow, FAC, and conductivity have a 2D topside relation given by Eq. 6.12 in Kelley (2009):

$$j_\parallel(x,y) = \Sigma_P \nabla\cdot\mathbf{E} + \mathbf{E}\cdot\nabla\Sigma_P + (\mathbf{E}\times\mathbf{b})\cdot\nabla\Sigma_H \quad (1)$$

where $j_\parallel$ is a horizontal map of FAC at the topside ionosphere, Σ_P and Σ_H are the height-integrated Pedersen and Hall conductivities, and $\mathbf{E}$ is the perpendicular ionospheric electric field.
- This 2D picture can significantly hide the 3D nature of auroral current closure.
- Due to the highly sensitive nature of auroral current closure to the 3D conductivity volume, how electron precipitation is defined is crucial.

Problem Statement

This work focuses on an important part of auroral arc systems: **impact ionization** imparted by **electron precipitation**. This flux is often assumed to be a simple unaccelerated Maxwellian. However, for discrete aurora, this flux can be a superposition of a primary accelerated Maxwellian population along with secondary, low energy population of re-accelerated backscatter (Evans, 1974). We investigate the bearing this has on auroral current closure by comparing **unaccelerated** vs. **accelerated** Maxwellian electron precipitation, both with and without the backscatter **low-energy tail**.

Ways to Define Electron Precipitation

- We look at three parallel differential electron number fluxes (see **Figure 1**):
  1. An **unaccelerated Maxwellian**:

$$J_\parallel(E;E_0) = \frac{Q_0}{2E_0^2}\frac{E}{E_0}\exp\left(-\frac{E}{E_0}\right) \quad (2)$$

  where Q_0 is the total energy flux, $Q_0 \equiv \int_0^\infty E J_\parallel(E)\,dE$, and E_0 is the characteristic energy.
  2. An **accelerated Maxwellian**:

$$J_\parallel(E;T_s,U_d) = \begin{cases} \dfrac{Q_0}{T_s^2+(T_s+U_d)^2}\dfrac{E}{T_s}\exp\left(-\dfrac{E-U_d}{T_s}\right), & E\geq U_d \\ 0, & \text{else}\end{cases} \quad (3)$$

  where T_s is the characteristic energy of the source region and U_d is the acceleration region potential drop (Kaeppler, 2013).
  3. A combination of a primary **accelerated Maxwellian** from the source region and a **low-energy tail** (LET) from re-accelerated backscattered electrons of ionospheric origin (Evans, 1974).

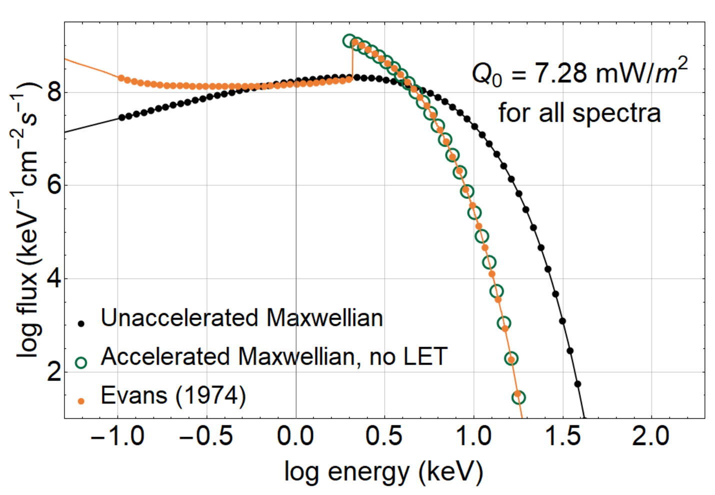

Figure 1: Three types of differential electron number fluxes: an unaccelerated Maxwellian with $E_0 = 2$ keV, an accelerated Maxwellian with $T_s = 800$ eV and $U_d = 2$ keV, and a transcribed flux from Fig. 5a by Evans (1974) assuming a 45° solid pitch angle. Points indicate energies used in composing ionization rates via calculations by Fang et al. (2010).

From Precipitation Spectra to Impact Ionization

- Calculations of altitude dependent impact ionization rates are done using two methods by Fang et al. (2008) and by Fang et al. (2010):
  - **Method A:** Fang et al. (2008) parameterize with isotropic, unaccelerated precipitation using both multistream (Lummerzheim & Lilensten, 1994) and two-stream (Solomon & Abreu, 1989) transport models.
  - **Method B:** Fang et al. (2010) do the same but with isotropic, monoenergetic precipitation which allows for building up arbitrary precipitation spectra using multiple of their calculations (see **Figure 2**).

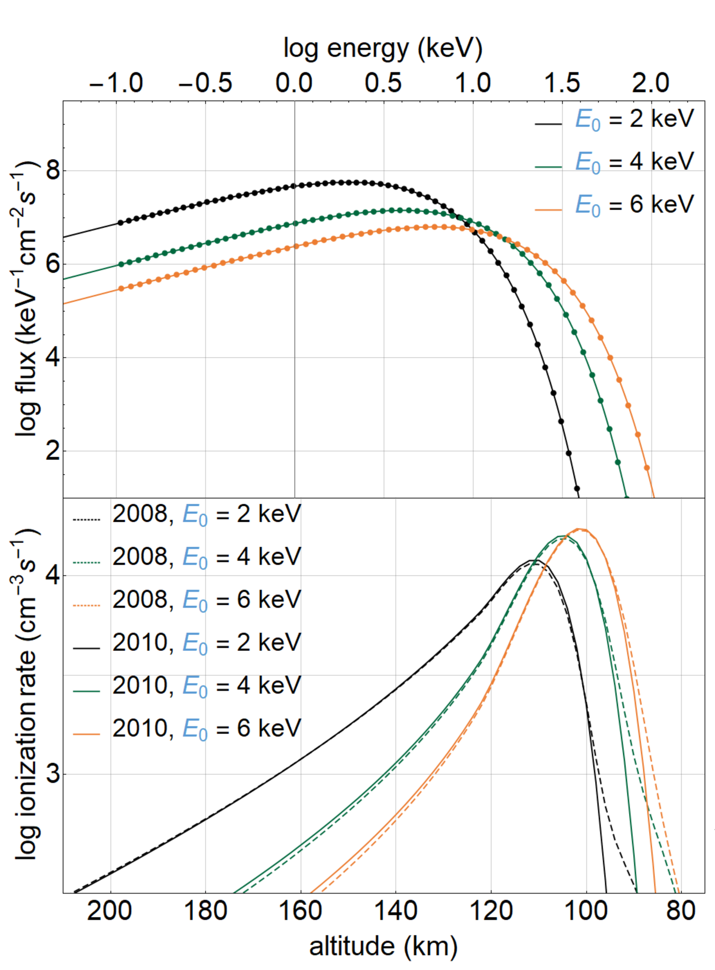

*Figure 2: A comparison of impact ionization rates using methods A and B. **Top:** Three unaccelerated Maxwellian spectra given by Eq. (2) with characteristic energies, E_0. Lines indicate the full spectra used in method A and points show what energies, E_{mono}, are used in composing the same spectra for method B. **Bottom:** Ionization rates vs. altitude calculated using method A (dashed) and method B (solid). This uses an MSISE-90 (Hedin, 1991) atmosphere at 10 UT on Feb 1, 2015, at 65.8° N and 207.7° E, with daily and 3-month-avg. F10.7 cm radio emissions of 143.7 and 137.6, and a daily Ap-index of 20.*

Accelerated vs. Unaccelerated Impact Ionization

- **Figure 3** shows how impact ionization altitude profiles change when comparing unaccelerated vs. accelerated Maxwellians.
- Defining an "X keV" auroral arc with either E_0 or U_d can change peak ionization rate altitudes by 10-20 kilometers.
- Depending on the source characteristic energy, T_s, an accelerated "4 keV" arc can vary peak ionization by 10-20 km in altitude.
- Only when $E_0 = U_d = T_s$ is an unaccelerated spectrum comparable to an accelerated one.

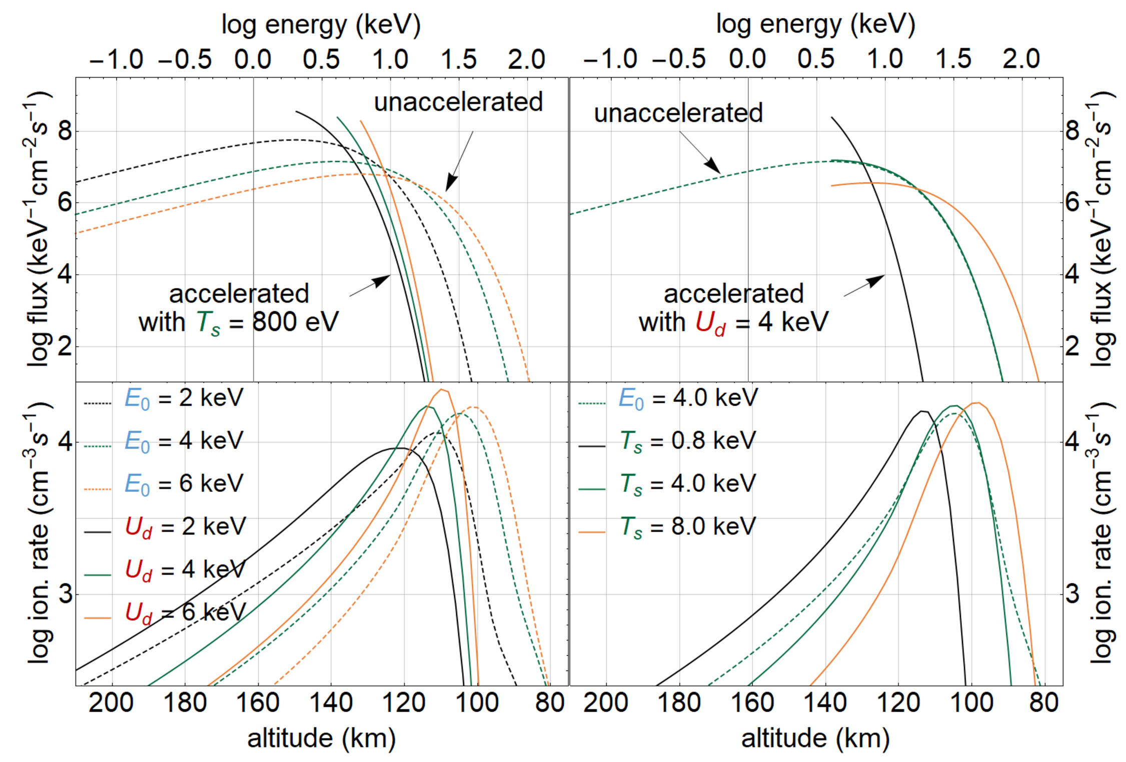

*Figure 3: **Left:** Unaccelerated (dashed) vs. accelerated with $T_s = 800$ eV (solid) spectra and resulting ionization rate altitude profiles for different peak flux energies. **Right:** Unaccelerated with $E_0 = 4$ keV (dashed) vs. accelerated with $U_d = 4$ keV (solid) for different source characteristic energies.*

Implementing Arbitrary Spectra into GEMINI

- To look at auroral current closure, we use multi-fluid model runs provided by GEMINI (Zettergren & Semeter, 2012; Zettergren & Snively, 2019). For details see github.com/gemini3d.
- This model can simulate the ionosphere at auroral arc scales (see **Figure 6**).
- GEMINI solves for static current continuity to account for changes in model parameters impacting conductivities as it steps forward in time.
- The model is forced with a 2D topside map of FAC or flow (see **Figure 7**).
- Additionally, in its present version, it is driven with 2D topside electron precipitation maps of Q_0 and E_0 covering impact ionization via method A.
- We implemented method B into GEMINI and tested it (see **Figure 4**).
- **Figure 5** shows GEMINI results after running the three spectra in Figure 1.

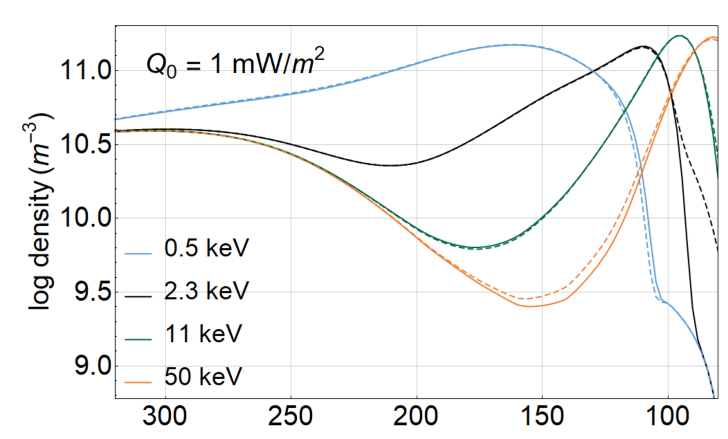

Figure 4: Example test of the implementation into GEMINI of method B (solid) against the original method A (dashed). These tests are done at 4 orders of magnitude in both E_0 and Q_0 ($Q_0 = 0.1, 10, 100$ mW/m^2 not shown).

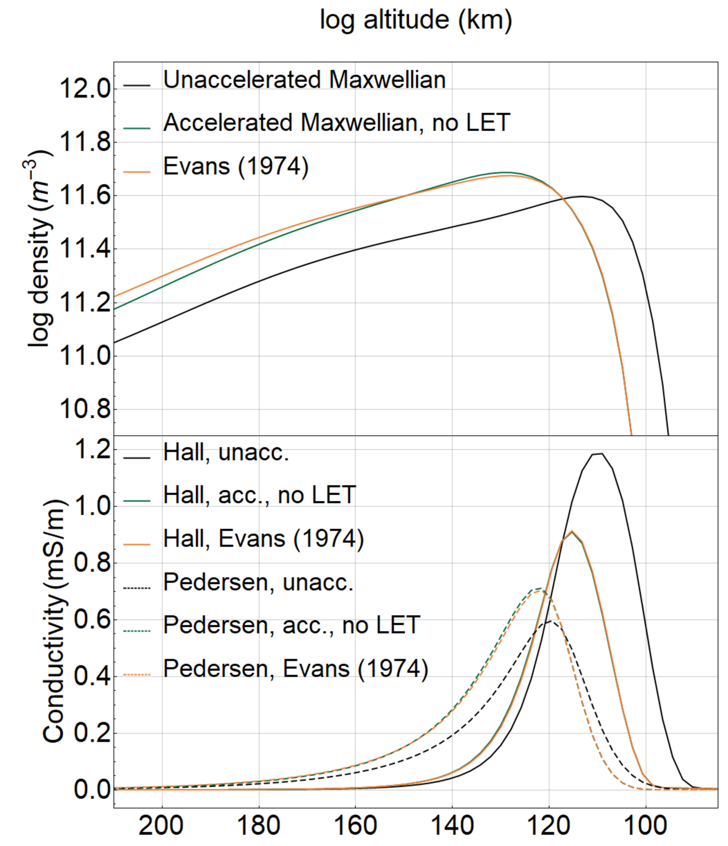

*Figure 5: GEMINI results for a 2D (alt., lat.) simulation with a topside line of constant precipitation as defined by the spectra in Figure 1 using method B. This simulation has no FAC or plasma flow drivers. **Top:** Electron density altitude profile for the three different spectra. **Bottom:** Hall (solid) and Pedersen (dashed) conductivity altitude profiles.*

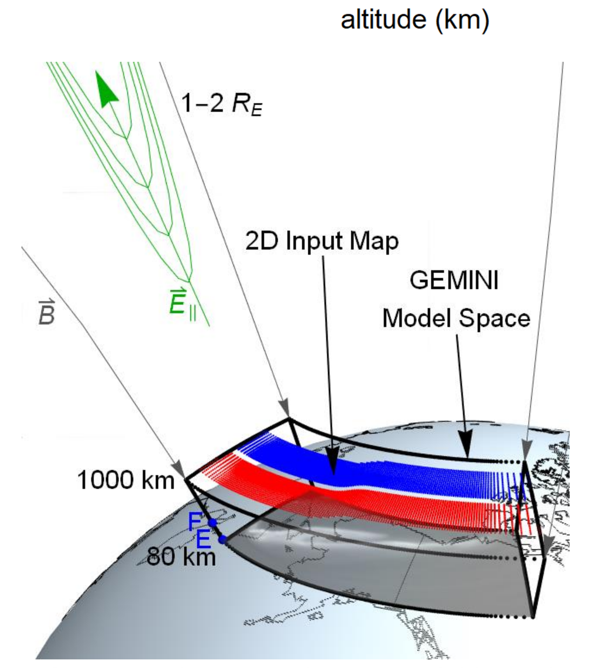

Figure 6: The general context of this work and the GEMINI model space.

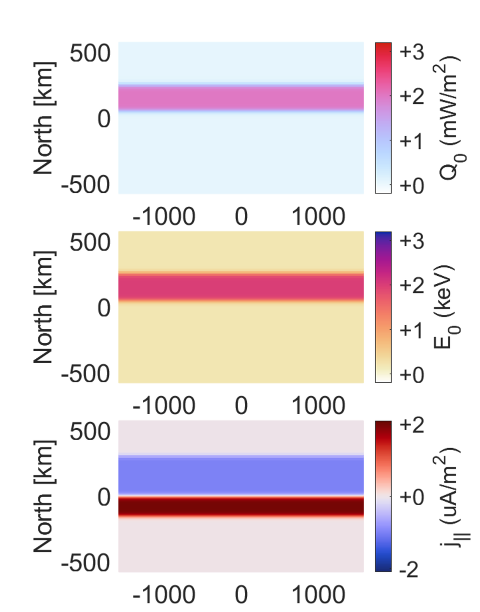

Figure 7: Typical topside 2D input maps for a GEMINI simulation.

Current Closure: Accelerated vs. Unaccelerated

- To visualize 3D current closure, we use current flux tubes made possible by the condition of static current continuity, $\nabla\cdot\mathbf{j} = 0$, enforced by GEMINI.
- Below are the results of four GEMINI simulations:
  - **A.** An unaccelerated Maxwellian with a 200 km wide arc of $E_0 = 2$ keV.
  - **B.** An accelerated Maxwellian with $U_d = 2$ keV and $T_s = 800$ eV and LET.
  - **C.** One with precipitation and FAC cut short with and without acceleration.
- All simulations have a 300 km wide sheet of 2 μA/m^2 FAC collocated with the arc, along with a 150 km, 4 μA/m^2 return sheet. The background precipitation is unaccelerated with $Q_0 = 0.3$ mW/m^2 and $E_0 = 1.5$ keV and they all use the same MSISE-90 values from Figure 2.

A

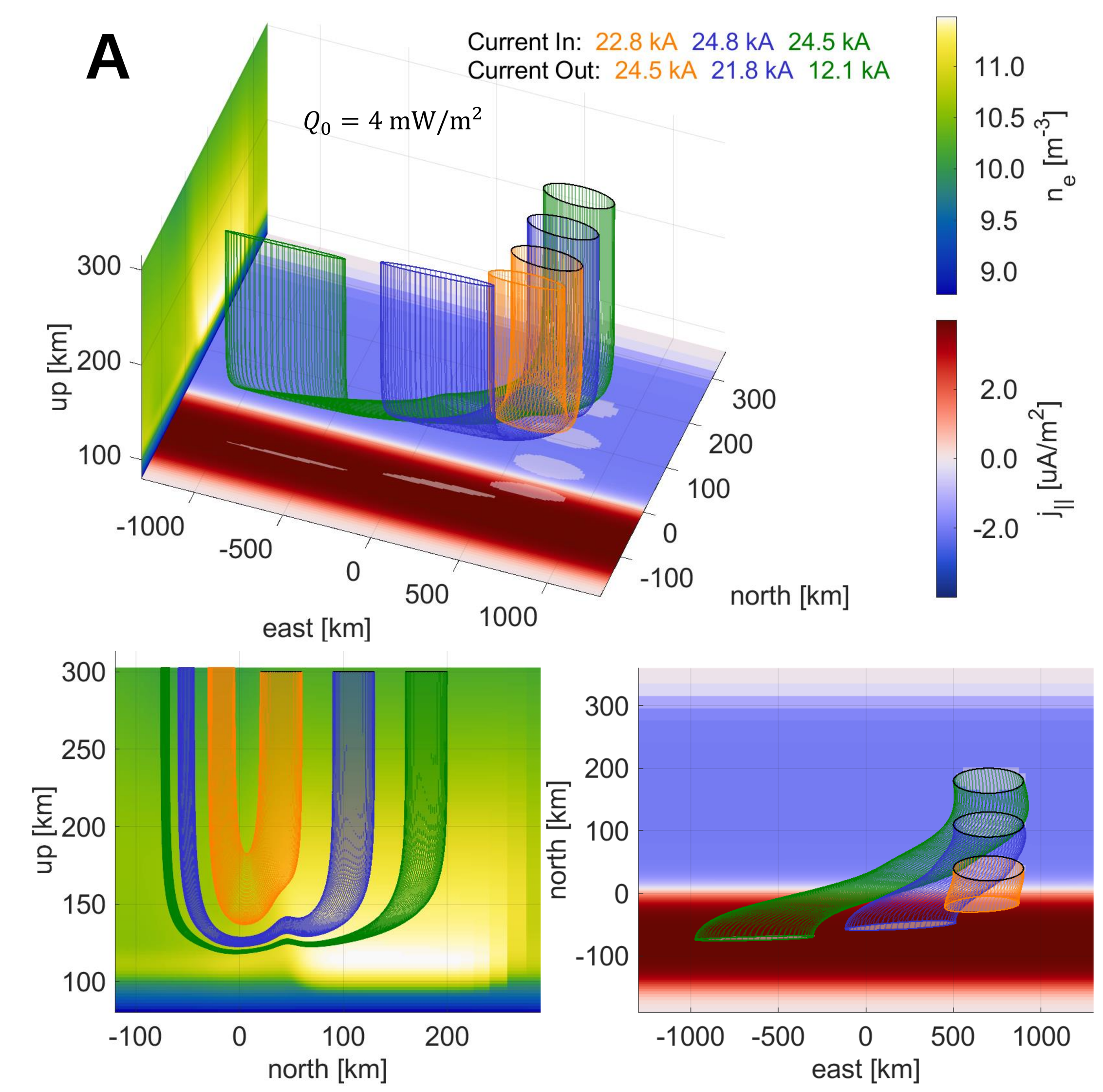

B

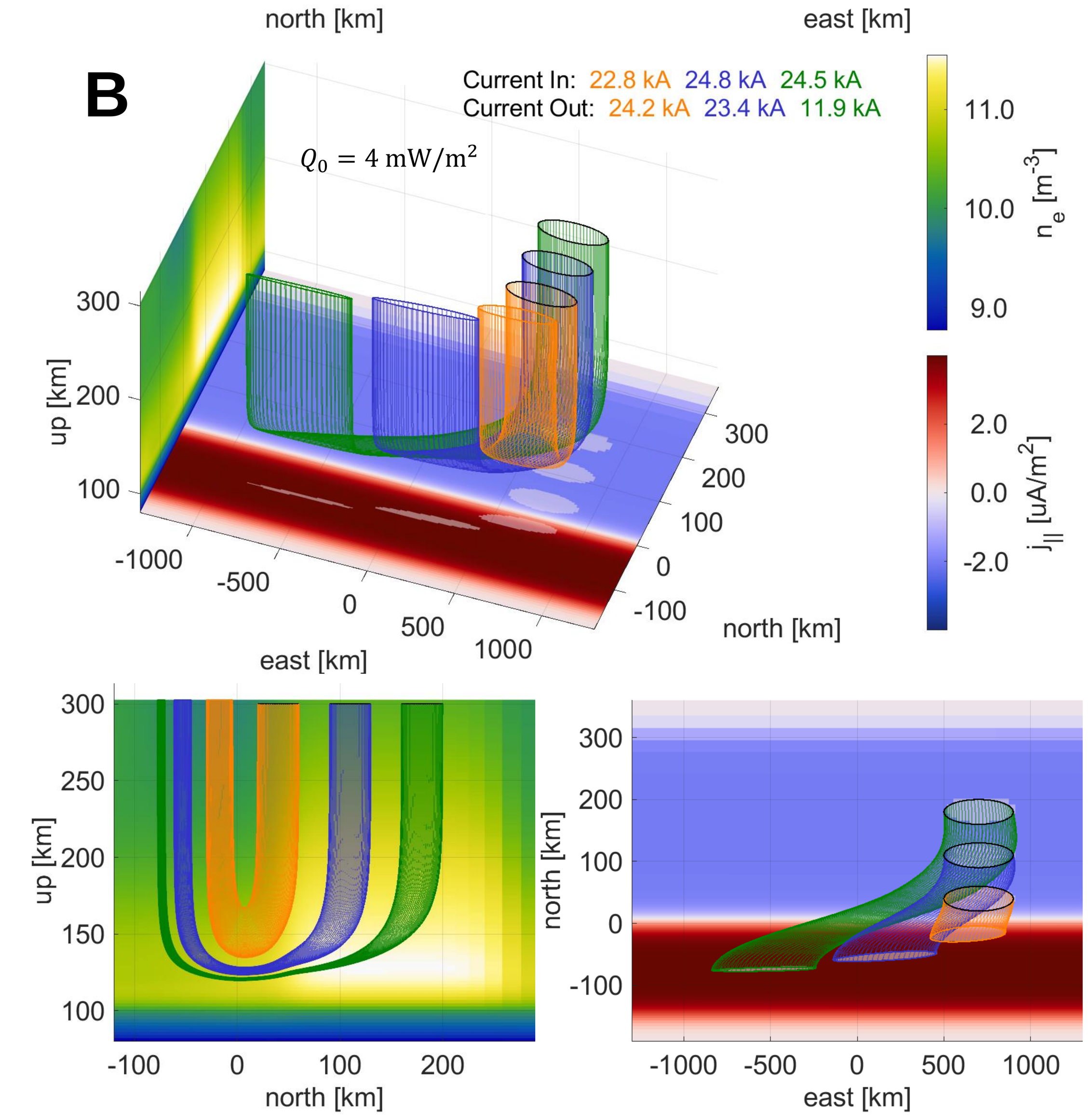

C

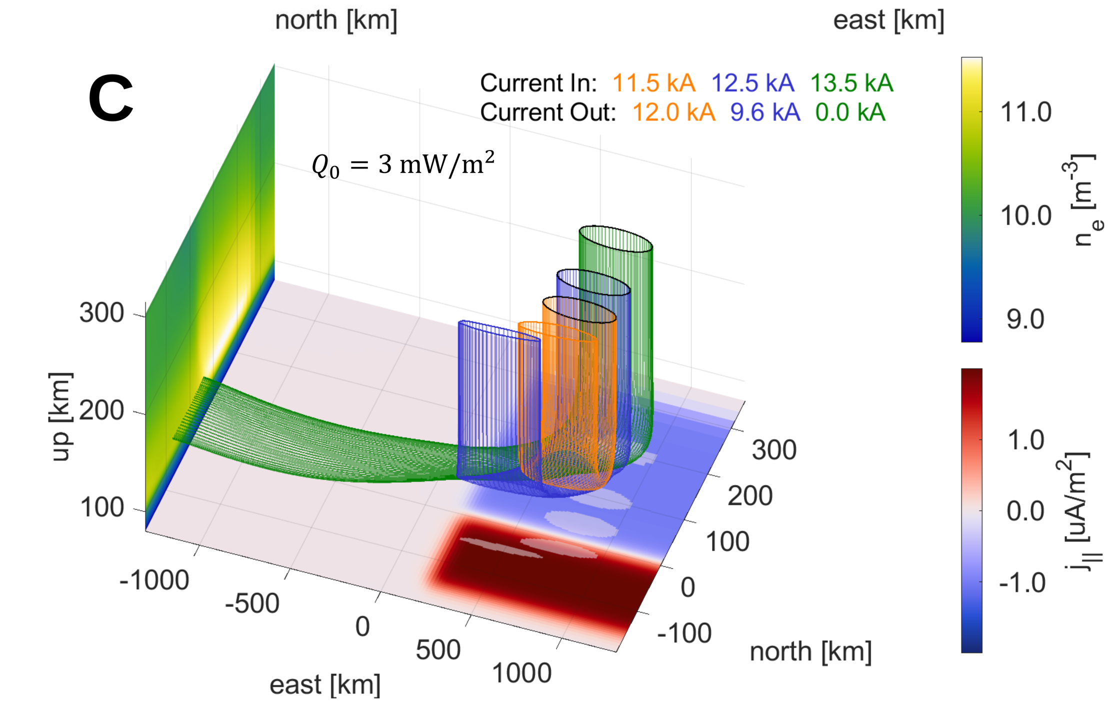

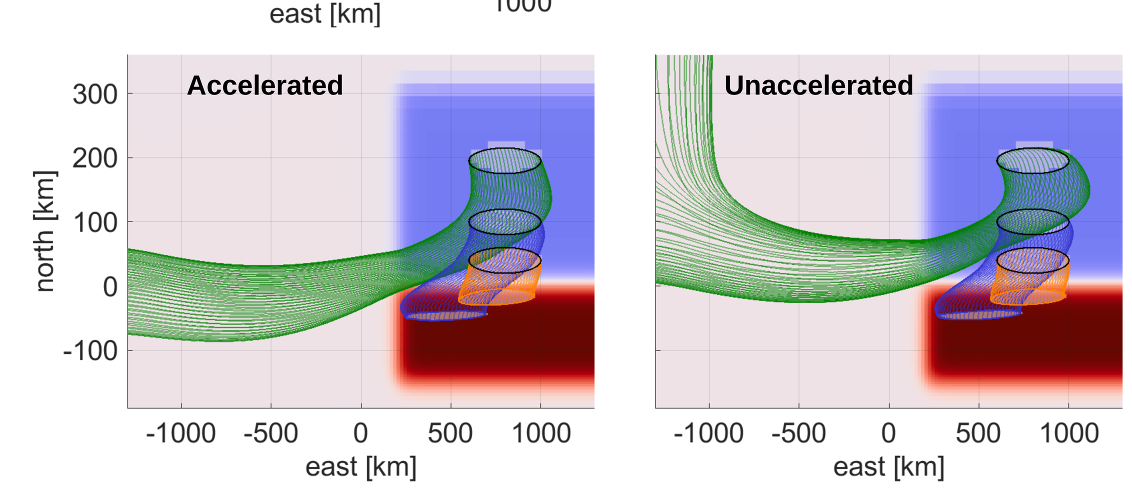

Discussions

- First and foremost, for the most basic example of an auroral system, the morphology of current closure is 3D in nature.
  - This is the interplay of the altitude-dependent Pedersen and Hall conductivities as current finds the path of least resistance.
- The scientific community may proxy auroral precipitation as unaccelerated Maxwellians when trying to conserve parameter space.
  - This assumption inadvertently makes the choice of hot source plasma.
  - When choosing Eq. (3) instead, you always have the choice of $U_d \to 0$.
- Using an unaccelerated Maxwellian when defining an auroral arc can significantly over- or underestimate the peak impact ionization altitude, on the order of the neutral scale height (~18 km).
  - This depends largely on the T_s/U_d ratio of the precipitation.
- The electron density and conductivity altitude profiles can change significantly when using accelerated vs. unaccelerated spectra.
  - The LET seems less significant in terms of auroral current closure.
- For accelerated spectra, current flux tubes can start closing at higher altitudes compared to unaccelerated spectra.
  - This is because more of the available precipitation energy is dumped at higher altitudes with a "colder" spectrum.
- Along-arc structures are expected to be more sensitive to choice of spectra.

Conclusions

- Even for the most basic auroral systems, a 2D description hides the 3D nature of current closure.
- Using unaccelerated Maxwellians when modelling discrete auroral arc systems is insufficient and an accelerated spectrum should be used instead.
- The low-energy precipitation tail caused by re-accelerated backscattered electrons (Evans, 1974) is relatively less important for auroral current closure.

Going Forward

- Now that we can choose any spectrum, we can construct broadband, Alfvénic precipitation as is done by Mella et al. (2011) (see **Figure 8**).
- Moving away from current closure, the choice of spectrum, especially the lower energies, also has strong effects on electron heating (see **Figure 9**), and in turn also effects ion upflow.
- Other possible sensitivities: energy balance/dissipation, Cowling channel (Cowling, 1932), neutral coupling.
- When doing all-sky imagery inversions, making the right choice of spectrum is crucial.

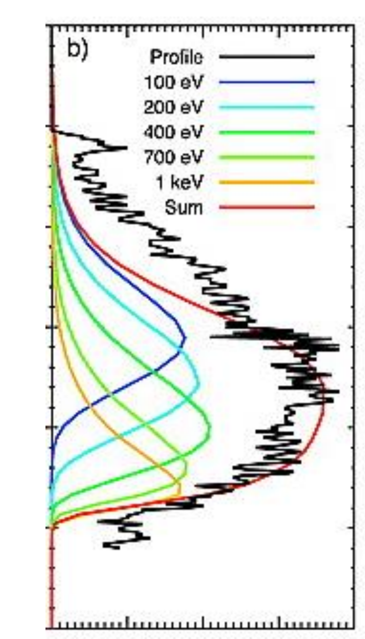

Figure 8: Fig. 11b by Mella et al. (2011): broadband light intensity profile constructed out of Maxwellians.

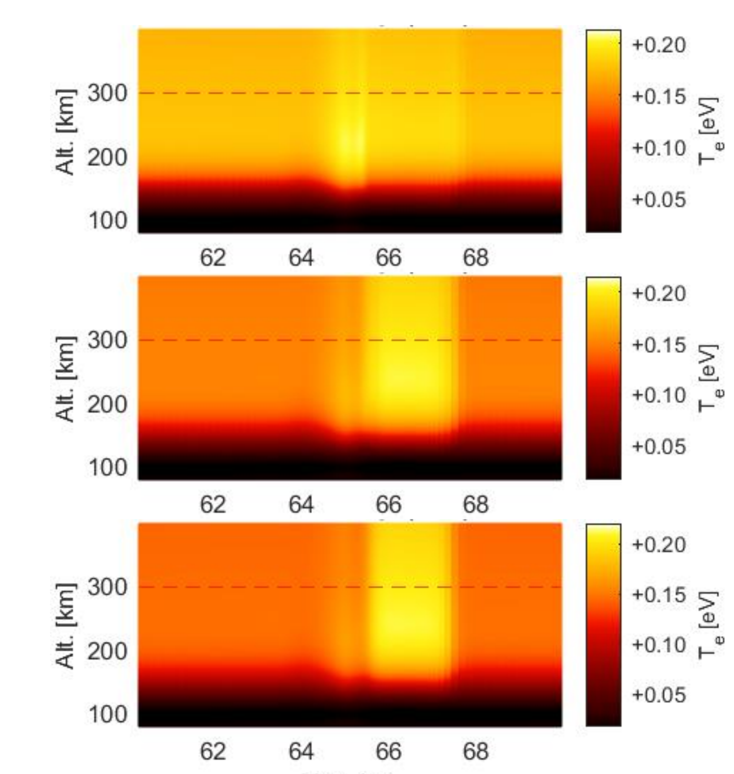

Figure 9: Electron temperature slices due to precipitation spectra that are unaccelerated, accelerated with no LET, and accelerated with LET.

Acknowledgements

We would like to thank M. Hirsch (B.U.) and T. Kovacs (Dartmouth College) for invaluable GEMINI technical support and M. Burleigh (NRL) for many insightful discussions. We would like to acknowledge and thank Dartmouth College for providing internal funding for Phase A of the Auroral Reconstruction Cube Swarm (ARCS) proposal and NASA 80GSFC21C0009 for the ARCS MIDEX CSR funding. We would also like to thank the NSF and NASA for providing funding for the GEMINI model development from grants NSF AGS1255181 and NASA NNX14AQ39G.

Scan for videos of current flux tubes and more!

References

Amm, O. et al., 2008, *Annales Geophysicae*, 10.5194/angeo-26-3913-2008
Cowley, S. W. H., 2000, *Geophysical Monograph Series*, 10.1029/GM118p0091
Cowling, T. G., 1932, *Mon. Not. R. Astron. Soc.*, 10.1093/mnras/93.1.90
Evans, D. S., 1974, *J. of Geophys. Research*, 10.1029/JA079i019p02853
Fang, X. et al., 2008, *J. of Geophys. Research*, 10.1029/2008JA013384
Fang, X. et al., 2010, *Geophysical Research Letters*, 10.1029/2010GL045406
Hedin, A. E., 1991, *J. of Geophys. Research*, 10.1029/90JA02125
Kaeppler, S. R., 2013, *U. of Iowa*, 10.17077/etd.vqmju27g
Kelley, M. C. et al., 2009, *Academic Press*, ISBN: 9780080916576
Lotko, W., 2004, *J. of Atmos. & Solar-Terrestrial Physics*, 10.1016/j.jastp.2004.03.027
Lummerzheim, D., & Lilensten, J., 1994, *Ann. Geophys.*, 10.1007/s00585-994-1039-7
Mella, M. R. et al., 2011, *J. of Geophys. Research*, 10.1029/2011JA016428
Solomon, S. & Abreu, V., 1989, *J. of Geophys. Research*, 10.1029/JA094iA06p06817
Wolf, R. A., 1975, *Space Science Reviews*, 10.1007/BF00718584
Zettergren, M. & Semeter J., 2012, *J. of Geophys. Research*, 10.1029/2012JA017637
Zettergren, M. & Snively J., 2019, *J. of Geophys. Research*, 10.1029/2018GL081569